

GREEDY THIELE CONTINUED-FRACTION APPROXIMATION ON CONTINUUM DOMAINS IN THE COMPLEX PLANE

TOBIN A. DRISCOLL* AND YUXING ZHOU†

Abstract. We describe an adaptive greedy algorithm for Thiele continued-fraction approximation of a function defined on a continuum domain in the complex plane. The algorithm iteratively selects interpolation nodes from an adaptively refined set of sample points on the domain boundary. We also present new algorithms for evaluating Thiele continued fractions and their accessory weights using only a single floating-point division. Numerical experiments comparing the greedy TCF method with the AAA algorithm on several challenging functions defined on the interval $[-1, 1]$ and on the unit circle show that continuum TCF is consistently 2.5–8 times faster than AAA.

Key words. approximation, rational functions, continued fractions, complex analysis

MSC codes. 65D15, 26C15, 11A55

1. Introduction. The use of rational functions, i.e., ratios of polynomials, for approximation is an old subject. But interest in their use as viable numerical objects began to grow rapidly in 2018, with the introduction of the AAA algorithm [10]. This method, based on the barycentric representation of rational functions, allows the construction of rational approximations to a function f defined on a set of sample points in the complex plane. The AAA algorithm adaptively selects a subset of n of the sample points as interpolation nodes and chooses n weights to minimize a linearized residual at the remaining sample points. The AAA algorithm has been extended in various ways [6, 17], and many applications of it are described in a forthcoming survey [12].

The AAA algorithm requires an SVD at each iteration, and building an interpolant on n nodes takes $O(n^4)$ work. In practice, the absolute running times are usually well under a second, but the high asymptotic cost is notable. It can be reduced by adopting updating [6] or random sketching [13] techniques, but these are not yet in widespread use.

Salazar Celis proposed [14] an alternative greedy iteration for rational approximation based on Thiele’s continued fraction (TCF) representation [15]. This method also adaptively selects nodes from a set of sample points, but it requires no linear algebra and an $O(n^3)$ cost to build an interpolant on n nodes. The method appears to be numerically stable in practice, although no proof of this is known.

Both AAA and the greedy TCF method were initially described in terms of fixed sample point sets in the complex plane. In some situations, however, ab initio discretization of the domain boundary is complicated by the presence of unknown nearby singularities in the function to be approximated. Driscoll et al. [4] described an adaptive refinement strategy for AAA that allows it to work on a continuum domain by adaptively refining the sample set.

In this paper, we propose a similar continuum strategy for the greedy TCF method. We also point out how to evaluate the TCF representation—and, by extension, the reciprocal differences analogous to barycentric weights—with a single floating-point division rather than $O(n)$ of them, resulting in practical speedups of 1.5x in the real case and over 5x in the complex case. We also point out that the evaluation is easily augmented to compute derivatives of the interpolant and its residues

*Department of Mathematical Sciences, University of Delaware, Newark, DE (driscoll@udel.edu).

†Department of Mathematical Sciences, University of Delaware, Newark, DE (zhouyx@udel.edu).

at simple poles.

In [section 2](#), we introduce the TCF representation and Salazar Celis' greedy algorithm. In [section 3](#), we describe the new adaptive refinement strategy for continuum domains. In [section 4](#), we present the new algorithms for evaluation, derivatives, and residues, and some elementary operations. In [section 5](#), we present numerical experiments comparing the greedy TCF method with AAA on several challenging functions defined on the interval $[-1, 1]$ and on the unit circle, demonstrating that TCF is consistently 2.5–12 times faster than AAA. Finally, in [section 6](#), we summarize our findings.

2. Thiele's continued fraction representation for rational interpolation.

Thiele [\[15\]](#) introduced a continued fraction representation for rational interpolation in 1909; the treatment in [\[9\]](#) is more accessible to English readers, and [\[14\]](#) is more modern. Given distinct real or complex nodes z_1, \dots, z_n at which to take values y_1, \dots, y_n , we define

$$(2.1) \quad r_n(z) = w_1 + \frac{z - z_1}{w_2} + \frac{z - z_2}{w_3} + \dots + \frac{z - z_{n-1}}{w_n},$$

where the weights w_k are implicitly defined via the interpolation conditions. Classically they are expressed as reciprocal divided differences; alternatively, inserting $y_k = r_n(z_k)$ into [\(2.1\)](#) and rearranging leads to the complementary continued fractions

$$(2.2) \quad w_k = 0 + \frac{z_k - z_{k-1}}{-w_{k-1}} + \dots + \frac{z_k - z_2}{-w_2} + \frac{z_k - z_1}{-w_1} + \frac{y_k}{1}, \quad k = 1, \dots, n.$$

If no indeterminate values are encountered in its construction, then $r_n(z)$ is a rational function that interpolates the given data. Generically (i.e., in the absence of cancelling factors), r_n is of rational type (m, m) if $n = 2m + 1$ and type $(m, m - 1)$ if $n = 2m$. Exceptions occur if one or more of the nodes is a so-called *unattainable* point, for which the interpolation at the specified degree is impossible. While theoretically interesting, such cases are rare in practice and easily detected [\[14\]](#).

A more substantive issue is the numerical stability of evaluations of r_n , which depends greatly on the locations and ordering of the nodes, as well as the values to be interpolated. Jones and Thron [\[8\]](#) recommended the tail-ordered evaluation $r_n(z) = v_1$ resulting from the iteration

$$(2.3) \quad \begin{aligned} v_n &= w_n, \\ v_k &= w_k + \frac{z - z_k}{v_{k+1}}, \text{ for } k = n - 1, \dots, 1. \end{aligned}$$

Graves–Morris [\[5\]](#) showed that a pivoting-style strategy of node ordering leads to a backward stable method, albeit with an upper bound containing a pessimistic exponential growth factor. Beckerman et al. [\[1\]](#) proved that pivoting and the growth factor are not necessary for some functions defined over real intervals.

Salazar Celis [\[14\]](#) suggested a different heuristic for ordering nodes. Given r_k interpolating at z_{i_1}, \dots, z_{i_k} , choose next the node with index

$$(2.4) \quad i_{k+1} = \arg \max_{1 < \nu \leq k} |r_k(z_{i_\nu}) - y_{i_\nu}|.$$

This greedy strategy, presented more formally in [Algorithm 2.1](#), parallels the AAA adaptive process. While no proof was offered of numerical stability, numerical evidence for challenging functions showed no signs of significant instability. We follow this approach and offer more evidence of stability in [section 5](#).

Algorithm 2.1 Discrete version of the greedy TCF algorithm.

Given: n -vector of sample points z , n -vector of corresponding values y , tolerance τ
 Initialize index vector $I \leftarrow [i]$ for some $1 \leq i \leq n$
 Error estimate $\epsilon \leftarrow \infty$
 $k \leftarrow 1$
while $\epsilon > \tau$ and $k \leq n$ **do**
 Calculate weight w_k using (2.2) with the last node/value pair from I
 $i \leftarrow \arg \max_{j \notin I} |r_k(z_j) - y_j|$ using (2.3)
 Append i to I
 $\epsilon \leftarrow |r_k(z_i) - y_i|$
 $k \leftarrow k + 1$
end while
return I, w

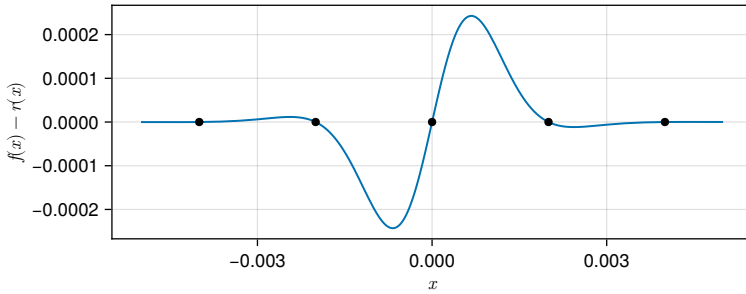


FIG. 3.1. Error in the interpolation of $f(x) = \arctan(500x)$ using 1001 sample points in the interval $[-1, 1]$. The discretization is too coarse near the origin, where the error is of size 2×10^{-4} .

3. Adaptive refinement for a continuum domain. In order to apply AAA or Algorithm 2.1 to approximate a function on a domain in the complex plane, the typical first step is to discretize the domain boundary. Since the computational effort of both algorithms scales linearly with the number of sample pairs provided, and because rational approximations themselves do not require special node distributions, there is often no need to choose the discretization too carefully—one can always oversample without significant cost. However, for functions with singularities very close to the boundary, more care may be needed, and these are the functions for which rational approximation offers the greatest advantage.

Figure 3.1 illustrates this problem for the function $f(x) = \arctan(500x)$ on an equispaced grid of 1001 points in the interval $[-1, 1]$. While Algorithm 2.1 finds a type (53, 53) interpolant with error less than 1.6×10^{-14} on the sample points, the discretization is too coarse near the origin, where the error is of size 2×10^{-4} .

In the extreme case of a function with a singularity on the domain, it is known that a tapered exponential distribution of nodes is ideal [16]. However, an optimal distribution is less clear for singularities that are merely nearby, and, in any case, foreknowledge of the singularity structure is not always available. Driscoll et al. [4] described an adaptive refinement strategy for AAA that expands the sample point set after each iteration, and a similar strategy can be applied to the greedy TCF algorithm.

Suppose the boundary of the domain is given by the parameterization $\gamma : [0, 1] \rightarrow \mathbf{C}$, and let m be a small positive integer. Algorithm 3.1 describes an adaptive refinement strategy to produce a node set $z_k = \gamma(t_k)$, $k = 1, \dots, n$ for interpolating f . The algorithm maintains a sorting permutation I for the elements of t and defines sample sets S_1, \dots, S_n by

$$(3.1) \quad S_j = \{t_{i_j} + i \frac{t_{i_{j+1}} - t_{i_j}}{m+1} : i = 1, 2, \dots, m\},$$

with the convention that $t_{i_{n+1}} = 1$. The permutation I can be updated when a new node is selected using $O(\log n)$ comparisons in a binary search. In an efficient implementation, the sample sets S_j can also be updated rather than generated on the fly, but those details are omitted from Algorithm 3.1 for brevity.

Algorithm 3.1 Continuum version of the greedy TCF algorithm.

```

Given: function  $f : \mathbf{C} \rightarrow \mathbf{C}$ , curve parameterization  $\gamma : [0, 1] \rightarrow \mathbf{C}$ , tolerance  $\tau$ ,
 $m \in \mathbf{N}$ 
 $t \leftarrow [0]$ 
 $I \leftarrow [1]$ 
Error estimate  $\epsilon \leftarrow \infty$ 
 $k \leftarrow 1$ 
while  $\epsilon > \tau$  do
   $z_k \leftarrow \gamma(t_k)$ 
   $y_k \leftarrow f(z_k)$ 
  Calculate weight  $w_k$  using (2.2)
   $(j, \sigma) \leftarrow \arg \max_{1 \leq j \leq k; \sigma \in S_j} |r_k(\gamma(\sigma)) - f(\gamma(\sigma))|$ 
  Append  $\sigma$  to  $t$ 
  Update sorting permutation  $I$ 
   $\epsilon \leftarrow |r_k(\gamma(\sigma)) - f(\gamma(\sigma))|$ 
   $k \leftarrow k + 1$ 
end while
return  $t, I, z, y, w$ 

```

Each evaluation of r_k in Algorithm 3.1 requires $O(k)$ operations, and there are $O(mk)$ such evaluations per iteration, so the total cost of the algorithm is $O(mn^3)$ operations, where n is the final number of nodes selected. In practice, as was done with AAA [2] we start with a moderately large value of $m = 15$ and decrease it with each iteration until reaching a steady value of $m = 3$. This allows for exponential refinement of nodes near singularities without excessive cost.

By comparison, if Algorithm 2.1 ultimately selects n out of N candidate nodes, its cost is $O(Nn^2 - n^3)$ operations. In practice, N is usually much larger than n and even than $10n$, so it is typically at least as expensive as the continuum version, which also affords the ability to adapt to singularities or high frequencies in the function being approximated.

4. New computational algorithms for the TCF representation. Here we note a few algorithms for working with TCF that appear to be not otherwise found in the literature.

4.1. Low-division iterations for weights and evaluation. There exist well-known alternatives to (2.3) for evaluation of a continued fraction [9]. Namely, the

TABLE 4.1

Timing results in nanoseconds per evaluation of a continued fraction (4.1) with normally distributed random coefficients a_k, b_k . Experiments were done in Julia 1.12.0rc1 on an Apple M4 Pro processor.

n	Real coefficients			Complex coefficients		
	Using (2.3)	Using (4.2)	Ratio	Using (2.3)	Using (4.2)	Ratio
25	75.4	48.4	1.6	450.0	73.6	6.1
30	90.0	57.6	1.6	543.3	87.5	6.2
35	105.1	66.8	1.6	638.1	96.2	6.6
40	120.3	76.1	1.6	727.2	109.9	6.6
45	134.7	85.4	1.6	817.0	120.8	6.8
50	149.8	94.4	1.6	911.5	134.1	6.8

continued fraction

$$(4.1) \quad \frac{p_n}{q_n} = b_0 + \frac{a_1}{b_1 + \frac{a_2}{b_2 + \dots + \frac{a_n}{b_n}}},$$

is equivalent to the product

$$(4.2) \quad \begin{bmatrix} p_n \\ q_n \end{bmatrix} = \begin{bmatrix} b_0 & 1 \\ 1 & 0 \end{bmatrix} \begin{bmatrix} b_1 & 1 \\ a_1 & 0 \end{bmatrix} \dots \begin{bmatrix} b_{n-1} & 1 \\ a_{n-1} & 0 \end{bmatrix} \begin{bmatrix} b_n \\ a_n \end{bmatrix},$$

which is meant to be evaluated from right to left—that is, tail-first—and using scalar variables. Our chief interest in this form is that it requires $n - 1$ scalar multiplications, $n - 1$ scalar add-multiply operations, and only one division, whereas (2.3) requires $n - 1$ divisions and $n - 1$ additions. Thus, (4.2) may be faster on a processor for which floating-point division takes much longer than an add-multiply.

For example, Table 4.1 shows timing results for evaluating (4.1) on random coefficients, with n ranging from 5 to 50, using both (2.3) and (4.2). The results show a consistent speedup of 30–35% using the one-division formula when the coefficients are real, and a speedup of over 6x when the coefficients are complex.

The evaluation of r_n from (2.3) is equivalent to (4.2) with $b_k = w_{k+1}$, $a_k = z - z_k$. Algorithm 4.1 summarizes the resulting iteration, with additional information returned for use in the next section. The evaluation of weights from (2.2) for the case $k = n$ is also equivalent to (4.2) with

$$(4.3) \quad a_k = \begin{cases} z_n - z_{n-k}, & 1 \leq k \leq n-1, \\ y_n, & k = n, \end{cases} \quad b_k = \begin{cases} 0, & k = 0, \\ -w_{n-k}, & 1 \leq k \leq n-1, \\ 1, & k = n. \end{cases}$$

4.2. Computation of derivatives and residues. Computation of r_n at a point via simple iterations makes it straightforward to compute r'_n as well. This can be done by automatic differentiation software, or explicitly, as indicated in Algorithm 4.1, whose return values provide $r_n = p_n/q_n$ and $r'_n = (p'_n q_n - p_n q'_n)/q_n^2$. The numerical stability of this formula is unknown.

Salazar [14] described generalized eigenvalue algorithms for finding the roots and poles of r_n . To our knowledge, there are no published algorithms for computing residues at the poles specialized to the TCF representation.

Algorithm 4.1 Evaluation of p_n , q_n , and their derivatives from (4.2).

Given: n -vector of nodes z , n -vector of weights w , evaluation point ζ

```

 $p \leftarrow w_n, q \leftarrow \zeta - z_{n-1}$ 
 $p' \leftarrow 0, q' \leftarrow 1$ 
for  $k = n-2$  to 1 do
   $[p', q'] \leftarrow [w_{k+1}p' + q', p + (z - z_k)p']$  (simultaneously)
   $[p, q] \leftarrow [w_{k+1}p + q, (z - z_k)p]$  (simultaneously)
end for
 $[p', q'] \leftarrow [w_1p' + q', p']$  (simultaneously)
 $[p, q] \leftarrow [w_1p + q, p]$  (simultaneously)
return  $p, q, p', q'$ 

```

If $r_n = p_n/q_n$, $q_n(\zeta) = 0$, $p_n(\zeta) \neq 0$, and $q'_n(\zeta) \neq 0$, then ζ is a simple pole of r_n with residue

$$(4.4) \quad \text{Res}(r_n, \zeta) = \frac{p_n(\zeta)}{q'_n(\zeta)}.$$

The values of $q'_n(\zeta)$ can be computed as shown in Algorithm 4.1.

4.3. Elementary operations on continued fractions. A few elementary operations can be performed on TCF expressions. Adding a constant c to (2.1), for example, is trivially equivalent to adding c to the weight w_1 . Multiplying by a constant c is not much harder:

$$(4.5) \quad c r_n(z) = c w_1 + \frac{z - z_1}{w_2/c} + \frac{z - z_2}{c w_3} + \dots,$$

with the pattern of alternating multiplication and division by c continuing throughout. Reciprocation is also fairly easy: provided that z_0 is not a node of $r_n(z)$, then

$$(4.6) \quad \frac{z - z_0}{r_n(z)} = 0 + \frac{z - z_0}{w_1} + \frac{z - z_1}{w_2} + \dots$$

is another Thiele continued fraction. Note that $1/r_n$ alone cannot always be expressed in the form (2.1), since it may be of type $(n-1, n)$.

In general, operations between TCFs cannot be expected to yield a result of a type reachable by a TCF. Instead, such operations are best done by resampling the result in a new adaptive iteration.

5. Computational experiments. Discrete and continuum versions of the AAA and greedy TCF algorithms have been implemented in the `RationalFunctionApproximation` package [3] in Julia. Here we present some experiments comparing their convergence rates and computational costs for several challenging functions defined on the interval $[-1, 1]$ and on the unit circle. The experiments in this section were done using version 0.2.7 of the `RationalFunctionApproximation` package in Julia 1.12.0rc2 on an Apple M4 Pro processor.

5.1. Interval. We considered six functions on the interval $[-1, 1]$:

- Singularity at $x = 0$: $f_1(x) = \sqrt{x}$, $f_2(x) = |x|$
- Singularity near $x = 0$: $f_3(x) = |x + 10^{-6}i|$, $f_5(x) = \arctan(10^6 x)$
- Singularity near $x = -1$: $f_4(x) = \log(x + 1 + 10^{-6})$

- Oscillatory: $f_6(x) = \cos(100x)$

Each was approximated using continuum variants of greedy TCF and AAA approximation up to degree 120 or a tolerance of 100 times machine epsilon. The maximum error was measured on the union of several point sets. Define

$$(5.1) \quad \begin{aligned} T_1 &= \left\{ -1 + \frac{2k}{10000} : k = 0, 1, \dots, 10000 \right\}, \\ T_2 &= \left\{ 2^{-0.1k} : k = 10, 11, \dots, 1000 \right\}. \end{aligned}$$

In order to check near all possible singularities, the validation set was defined as $T_1 \cup T_2 \cup -T_2 \cup (T_2 - 1)$. Note that not only are these points more finely distributed throughout the interval than the points used within the algorithms, but they get much closer to $x = 0$ and $x = -1$ than is possible for the continuum algorithms to sample by repeated refinement in double precision. Convergence was measured as a function of the denominator degree, which allows two cases at each degree for TCF (numerator degree equal to or one greater than the denominator degree) and one case at each degree for AAA (balanced degrees only).

[Figure 5.1](#) shows the convergence results. Approximants that had true poles—that is, those with a nontrivial residue—in the domain are marked in red. These cases indicate that the iteration should not be stopped there but otherwise cause no practical difficulties. Overall, the two methods are quite comparable in convergence. In the two test functions with a singularity at $x = 0$, the convergence is root-exponential. In the cases with a singularity near the interval, exponential convergence is observed. The convergence for f_6 is stagnant until the function is sufficiently resolved, after which it is superexponential due to the lack of singularities.

The dashed lines on each plot represent the error achieved by discrete variants of the algorithms using a sample set consisting of the points in the validation set that can be distinguished in double precision. Thus, the discrete versions have access to exponentially refined points near any singularities, and we can check how well the continuum versions are able to find such points automatically. In all cases except f_5 for AAA, the continuum accuracy is comparable to or better than the discrete accuracy. Some additional experiments (not shown) indicate that this disappointing case can be repaired by increasing the steady value of the refinement level m in [Algorithm 3.1](#) from 3 to 4; this behavior seems particular to the choice of 10^6 in the definition of f_5 .

[Table 5.1](#) shows the elapsed construction times for both methods on these functions. To make the comparisons fair, each algorithm is run for the smaller of the number of iterations shown in [Figure 5.1](#) and the number needed to get as small an error as the best error achieved by the other method. Each construction was run 5 times to minimize variability. The greedy TCF method was found to be consistently faster by a factor ranging from 3.0 to 9.5. We note that a significant amount of the code and execution time is due to manipulating the sample points and iteration, particularly for TCF, even though care was taken to reduce unnecessary work duplication and memory allocation.

5.2. Unit circle. We considered six functions on the unit circle $|z| = 1$:

- Singularity at $z = -1$: $f_1(z) = \sqrt{1+z}$, $f_2(z) = |1+z|$
- Singularity near $z = -1$: $f_3(z) = |1+z+10^{-6}|$, $f_4(z) = \log(1+z+10^{-6})$,
 $f_5(z) = \sqrt{1+10^6-z^2}$
- Oscillatory: $f_6(z) = z^{50}$

The max error for each approximation was measured on the set

$$\cos(\pi T_1) \cup -\cos(\pm\pi T_2),$$

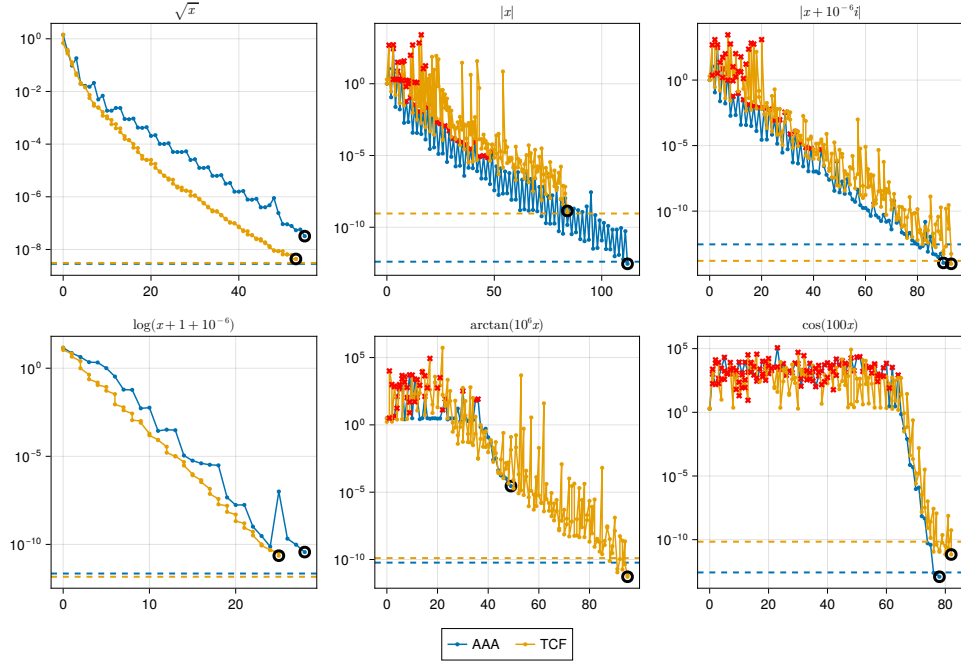


FIG. 5.1. Comparison of TCF and AAA approximation on the interval $[-1, 1]$ for six challenging functions. Each plot shows the max-norm error on a validation set described in the text as a function of the denominator degree. The black rings indicate the best approximation found for each run. Any approximation that has a genuine pole within the interval is marked with a red x . The dashed lines indicate the best approximation found by discrete variants of the algorithms.

where T_1 and T_2 are given in (5.1), which allows measurement of error close to a possible singularity at $z = \pm 1$. Unlike T_2 , however, the points in $\cos(\pi T_2)$ cannot all be distinguished in double precision, so the effective upper bound for k in the definition (5.1) is 520 rather than 1000.

The results are given in Figure 5.2 and Table 5.2. As on the unit interval, the convergence rates are similar for the two methods, while the ratios of computational times are all at least 3.1, and usually considerably larger. The continuum versions are able to achieve errors comparable to the discrete versions in all cases.

6. Concluding remarks. The barycentric representation of a rational function allows specifying n interpolation conditions along with n weights that are used to minimize a linearized residual at sample points in a least-squares sense. The result is a rational function of type $(n-1, n-1)$. By contrast, the Thiele continued-fraction representation works only with $2n$ or $2n+1$ interpolation conditions to produce a rational approximant with denominator degree n . Both representations can be combined with iterative greedy node selection, either on a predetermined discrete set of candidate nodes or on a continuum domain via adaptive refinement. Even though the TCF representation only “knows about” the function at the selected interpolation nodes, while the barycentric representation explicitly incorporates information from additional sample points, the two methods appear to have similar global convergence rates in our tests.

TABLE 5.1

Timing results for finding common best interpolants from those shown in Figure 5.1.

Function	AAA (msec)	TCF (msec)	Ratio
\sqrt{x}	31.0	3.4	9.1
$ x $	19.3	7.5	2.6
$ x + 10^{-6}i $	55.5	11.1	5.0
$\log(x + 1 + 10^{-6})$	1.7	0.6	3.0
$\arctan(10^6 x)$	35.3	4.7	7.5
$\cos(100x)$	34.7	6.8	5.1

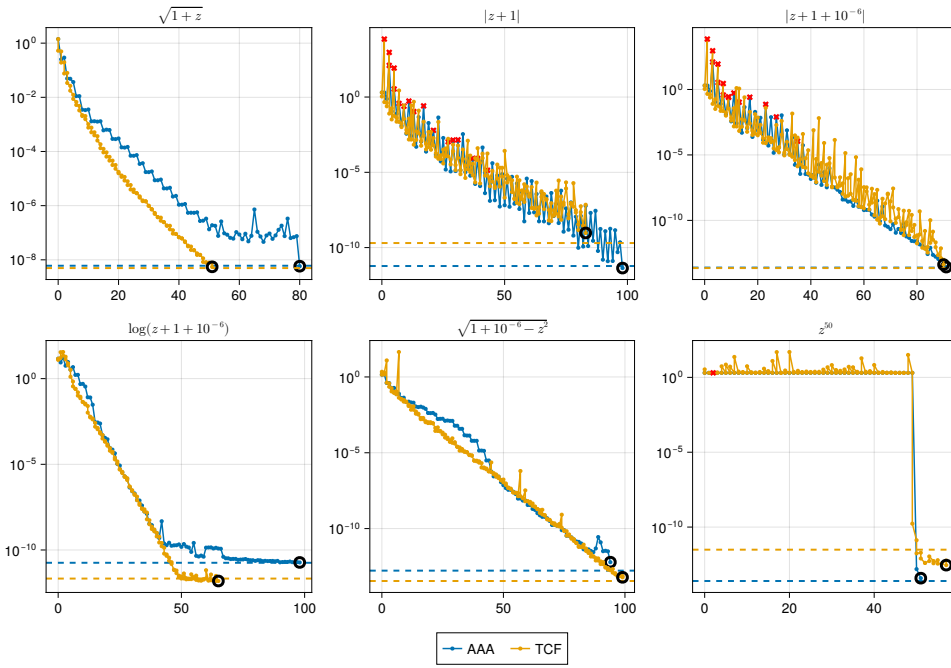


FIG. 5.2. Comparison of greedy TCF and AAA approximation on the unit circle for six challenging functions. Each plot shows the max-norm error on a validation set described in the text as a function of the denominator degree. The black rings indicate the best approximation found for each run. Any approximation that has a genuine pole on the circle is marked with a red x . The dashed lines indicate the best approximation found by discrete variants of the algorithms.

TABLE 5.2

Timing results for finding common best interpolants from those shown in Figure 5.2.

Function	AAA (msec)	TCF (msec)	Ratio
$\sqrt{1+z}$	78.7	3.8	20.6
$ 1+z $	77.7	13.9	5.6
$ 1+z+10^{-6} $	118.9	19.7	6.0
$\log(1+z+10^{-6})$	152.8	2.9	52.3
$\sqrt{1+10^{-6}-z^2}$	131.1	18.0	7.3
z^{50}	16.8	4.9	3.4

Evaluation of the rational approximant and its derivative is $O(n)$ for both representations. Finding its poles requires the solution of a generalized eigenvalue problem in either case. We have shown how to find the residue at a pole in $O(n)$ operations for the TCF representation. (The same should be possible for the barycentric representation using explicit or automatic differentiation for the denominator.) We have also shown how to perform a few elementary operations on the TCF representation, although more complicated operations are best done by resampling of the result.

The mode of premature failure observed for both discrete and continuum greedy TCF (such as for $|x|$ in Figure 5.1 and $|1+z|$ in Figure 5.2) is underflow during the computation of p_n and q_n from (4.2) for the weight associated with adding a new node. While the underflow can easily be detected and averted by a simple rescaling, doing so offers no convergence benefit in our experience, due to an associated cumulative loss of precision during the iteration due to subtractive cancellation. This can partly, but not entirely, be attributed to differences between the nodes as defined in (4.3). It is possible that representing the nodes by their consecutive differences, or a clever manipulation of the product of matrices in (4.2), could improve the situation.

The TCF representation requires no linear algebra and is remarkably simple in concept and implementation. The chief appeal of greedy TCF over AAA is its lower asymptotic work requirement by a factor $O(n)$ for construction. This advantage is offset somewhat by needing twice as many iterations to reach the same degree and the fact that a significant portion of the overall computation time is devoted to other tasks, such as memory management and refinement of the domain. In practice, our implementation finds the TCF method consistently faster on all of our test functions by a factor of at least 2.5 and typically between 3 and 8. This speed advantage is likely to be even more pronounced in extended-precision arithmetic, where efficient linear algebra is not always available.

In addition to the standard algorithm based on least-squares approximation, AAA offers a fast modification to find near-best approximations in the minimax sense through iterative reweighting [11]. Salazar Celis [14] demonstrated a near-best method using an equilibration algorithm [7], but its robustness and performance are unclear at present. AAA also has a long record of stable use for applications and successful modifications for exploiting symmetry and special problem types. The comparative simplicity and speed of TCF suggest that it is worth further investigation and development along similar lines.

Acknowledgments. We thank Nick Trefethen and Oliver Salazar Celis for helpful discussions and suggestions.

REFERENCES

- [1] B. BECKERMANN, J. BISCH, AND R. LUCE, *On the rational approximation of Markov functions, with applications to the computation of Markov functions of Toeplitz matrices*, Numerical Algorithms, 91 (2022), pp. 109–144, <https://doi.org/10.1007/s11075-022-01256-4>.
- [2] T. DRISCOLL, Y. NAKATSUKASA, AND L. N. TREFETHEN, *AAA rational approximation on a continuum*, 2023, <https://doi.org/10.48550/ARXIV.2305.03677>.
- [3] T. A. DRISCOLL, *RationalFunctionApproximation.jl: Rational function approximatoin in Julia*. Zenodo, Sept. 2023, <https://doi.org/10.5281/ZENODO.8355790>.
- [4] T. A. DRISCOLL, Y. NAKATSUKASA, AND L. N. TREFETHEN, *AAA Rational Approximation on a Continuum*, SIAM Journal on Scientific Computing, 46 (2024), pp. A929–A952, <https://doi.org/10.1137/23M1570508>.
- [5] P. R. GRAVES-MORRIS, *Practical, Reliable, Rational Interpolation*, IMA Journal of Applied Mathematics, 25 (1980), pp. 267–286, <https://doi.org/10.1093/imamat/25.3.267>.
- [6] A. HOCHMAN, *FastAAA: A fast rational-function fitter*, in 2017 IEEE 26th Conference on

Electrical Performance of Electronic Packaging and Systems (EPEPS), Oct. 2017, pp. 1–3, <https://doi.org/10.1109/EPEPS.2017.8329756>.

- [7] C. HOFREITHER, *An algorithm for best rational approximation based on barycentric rational interpolation*, Numerical Algorithms, 88 (2021), pp. 365–388, <https://doi.org/10.1007/s11075-020-01042-0>.
- [8] W. B. JONES AND W. J. THRON, *Numerical stability in evaluating continued fractions*, Mathematics of Computation, 28 (1974), pp. 795–810, <https://doi.org/10.1090/S0025-5718-1974-0373265-5>.
- [9] L. MILNE-THOMPSON, *The Calculus of Finite Differences*, Macmillan and Company, 1933.
- [10] Y. NAKATSUKASA, O. SÈTE, AND L. N. TREFETHEN, *The AAA algorithm for rational approximation*, SIAM Journal on Scientific Computing, 40 (2018), pp. A1494–A1522, <https://doi.org/10.1137/16m1106122>.
- [11] Y. NAKATSUKASA AND L. N. TREFETHEN, *An algorithm for real and complex rational minimax approximation*, SIAM Journal on Scientific Computing, 42 (2020), pp. A3157–A3179, <https://doi.org/10.1137/19M1281897>.
- [12] Y. NAKATSUKASA AND L. N. TREFETHEN, *Applications of {AAA} Rational Approximation*, Acta Numerica, (2025), p. to appear.
- [13] T. PARK AND Y. NAKATSUKASA, *A fast randomized algorithm for computing an approximate null space*, BIT Numerical Mathematics, 63 (2023), p. 36, <https://doi.org/10.1007/s10543-023-00979-7>.
- [14] O. SALAZAR CELIS, *Numerical Continued Fraction Interpolation*, Ukrainian Mathematical Journal, 76 (2024), pp. 635–648, <https://doi.org/10.1007/s11253-024-02344-5>.
- [15] T. N. THIELE, *Interpolationsrechnung*, Nineteenth Century Collections Online: Science, Technology, and Medicine, Part I, B.G. Teubner, Leipzig, 1909.
- [16] L. N. TREFETHEN, Y. NAKATSUKASA, AND J. A. C. WEIDEMAN, *Exponential node clustering at singularities for rational approximation, quadrature, and PDEs*, Numerische Mathematik, 147 (2021), pp. 227–254, <https://doi.org/10.1007/s00211-020-01168-2>.
- [17] L. N. TREFETHEN AND H. D. WILBER, *Computation of Zolotarev Rational Functions*, SIAM Journal on Scientific Computing, (2025), pp. A2205–A2220, <https://doi.org/10.1137/24M1687960>.